

XPS and IR spectral studies on the structure of phosphate and sulphate modified titania – A combined DFT and experimental study

K Joseph Antony Raj^a, R Shanmugam^b, R Mahalakshmi^b & B Viswanathan^{a,*}

^aNational Centre for Catalysis Research, Indian Institute of Technology Madras, Chennai 600 036, India
Email: bvnathan@iitm.ac.in

^bPG & Research Department of Chemistry, Thiagarajar College, Madurai 625 009, India

Received 30 October 2009; revised and accepted 14 December 2009

The structures of phosphated titania and sulphated titania are studied with a combined approach using DFT/B3LYP/LanL2DZ and experimental studies such as XRD, XPS, and DRIFT spectra. The infrared absorptions, Mulliken charges, bond lengths, and dipole moments are investigated for the phosphated and sulphated titania structures optimized by DFT calculations. The XRD patterns obtained for both the modified titania show that the as-synthesized materials are amorphous in nature. The DRIFT spectra show the presence of bidentate complex in both sulphated and phosphated titania. The XPS data show the presence of Ti-O-S and Ti-O-P linkages in sulphated and phosphated titania respectively. The evaluation of IR absorptions obtained by DFT and DRIFT spectra reveal the most favorable structure of bridged bidentate for sulphated titania and a combination of monodentate and chelating bidentate for phosphated titania.

Keywords: Theoretical chemistry, Density functional calculations, Catalysts, Spectral studies, X-ray diffraction, X-ray photoelectron spectroscopy, DRIFT spectroscopy, Titania, Phosphated titania, Sulphated titania

IPC Code: Int. Cl.⁹ B01J21/00

Titania has a number of technological uses, including in catalysis and photocatalysis. The anatase form of titania is used for wider applications than the rutile form as anatase appears to be catalytically active^{1,2}. Efforts have been made to refining the preparation and synthesis of anatase-TiO₂ with the goal of continuous improvement of its textural and acidic properties. Studies using density functional theory (DFT) on anatase-TiO₂³⁻⁹ provide insight into their acid-base properties under reacting conditions. Hetero atom doped titania has received considerable attention as a material for its photocatalytic activity. Since doping of elements can efficiently extend the photoresponse of TiO₂ to the low-energy region¹⁰, a substantial amount of research has focused on improving the absorption of visible light by doping with N¹¹, S¹², and F¹³. Asahi *et al.*¹⁴ have studied the effect of hetero atom doping in titania. Umebayashi *et al.*¹⁵⁻¹⁷ have suggested that S is substituted in the positions of oxygen or titanium in the titania lattice. It is generally believed that there are various possible configurations or chemical environments for nitrogen in N-doped TiO₂, as suggested by the multiple features observed by XPS^{18,19}. The relative abundance of the various N-containing species essentially depends on the method and conditions of synthesis of

the doped sample. Two recent reviews have summarized some of the facets of first (undoped) and second generation (doped) titania samples^{20,21}. Oliver *et al.*²² have investigated the adsorption, diffusion and desorption of chlorine on the partially reduced titania using DFT calculations. Gao *et al.*²³ have studied the incorporation of nitrogen in anatase TiO₂ by the first-principles calculations based on the DFT. Raghunath *et al.*²⁴ have reported the result of a density functional theory study on the adsorption and decomposition pathways of phosphorous acid on TiO₂ anatase (101) and rutile (110) surfaces.

Some studies report the preparations of sulphated²⁵ and phosphated titania²⁶ (ST and PT respectively). These S and P modified titania samples show the characteristics of high surface area and low crystallinity which demonstrates the incorporation of S and P in the framework of titania. A few reports^{27, 28} suggest bidentate structure of phosphates and sulphates on the surface of titania. The catalytic activity studies^{29,30} have shown remarkable performance of sulphate and phosphate modified titania. With the goal to clarify the reason for these observations, we report herein a combined theoretical and experimental study of sulphate and phosphate modified titania. The present work deals with the

determination of the structure of phosphated and sulphated titania using DFT studies. The various possible structures are taken as input for the DFT calculations. The obtained structure as output and its IR data have been analysed with the experimental DRIFT spectra and thereby the best possible structure is determined. The effect of removal of phosphates and sulphates from the surface of titania on heat treatment have been experimentally studied using XRD. XPS has been used to determine the oxidation state of P in PT and S in ST. In addition the environment of Ti and O in PT and ST has been analysed by XPS.

Methodology

Computational details

Quantum chemical computations were performed on the structures of phosphate and sulphate modified titania samples in order to find their IR absorptions and dipole moments and thereby the best possible structure. The molecular geometries of the model structures were fully optimized by density functional theory using Gaussian 03 software on a IBM p-series server without any geometrical restrictions. Gauss view 3.0³¹ was used as a graphical user interface. The effects of electron correlation on the geometry optimization were taken into account by using Becke's three parameter exchange functional with Lee-Yang-Parr gradient-corrected correlation functional (B3LYP)³² in conjunction with the Los Alamos ECP plus DZ basis sets (Lan12DZ)³³. The molecular structures of the systems with the highest symmetries were obtained by complete structural optimization. At the optimized geometries, the vibrational frequencies were calculated to ascertain that the structures correspond to potential minimum. Calculated frequencies are reported without any additional scaling factors. The obtained structures are shown in Figs 1 and 2.

Synthesis and characterization

The sulphated titania was prepared by hydrolyzing titanium oxysulphate in the presence of ammonia. The detailed procedure for the preparation of sulphated titania and phosphate modified titania are reported elsewhere³⁴.

Wide-angle XRD patterns for the calcined materials were measured using a Rigaku Miniflex II, using CuK α irradiation. The DRIFT spectra for the samples were recorded using Bruker Tensor-27. The XPS was recorded on a Omicron spectrometer in the

range of 0 - 800 eV. Photoelectron lines of the main constituent elements, O1s, Ti2p, S2p, P2s, and P2p, were recorded at 50 eV pass energy by 0.1 eV steps and with a minimum 200 μ s dwell time. All binding energies were referenced to the C1s peak at 284.4 eV.

Results and Discussion

X-ray diffraction

The XRD patterns of the phosphate modified titania (PT), sulphate modified titania (ST), crystalline anatase (Fluka) and its calcined samples at various temperatures are shown in Fig. 3. The XRD patterns show the presence of only the anatase phase in the PT and ST samples, irrespective of the calcination temperature. The PT and ST samples calcined at temperatures 500 and 900 °C in air for two hours show increasing crystallinity ranging from 31 to 63% with temperature for ST. PT shows no significant change in crystallinity with calcination temperature, demonstrating its thermal stability and strong adsorption of phosphate on the surface of titania. In addition, the crystallinity values suggest that PT is more stable than ST. The crystallinity of the samples was calculated using a standard anatase based on the intensity of XRD peak obtained at a 2θ of 25.3°. The prepared ST and PT samples dried at 100 °C showed a crystallinity of about 10% and consequently are considered as non-crystalline materials. In addition, the effect of substitution or adsorption of sulphates and phosphates on any particular plane on the surface of titania has not been considered for this study. Based on this assumption the possible structures of PT and ST samples are shown in Figs 1 and 2, for the prepared samples dried at 100 °C.

X-ray photoelectron spectra

The X-ray photoelectron spectra were employed to examine the oxidation state and the bonding characteristics of PO₄³⁻ and SO₄²⁻ on the surface of titania. The high resolution XPS of P2p, Ti2p and O1s core electrons on the surface of anatase and PT are shown in Fig. 4(a) - (c). The P/Ti ratio at the surface was determined to be 0.09 for P-TiO₂. The phosphated titania exhibits a binding energy for P2p at 134.5 eV, indicating that phosphorus in the sample exists in pentavalent-oxidation state and apparently as P-O bonded species³⁵. Absence of the characteristic binding energy of P in TiP at 128.6 eV indicates that Ti-P are not present in the sample³⁶. The peak at 134.5 eV has a binding energy similar to that of NaH₂PO₄ (133.9 eV)³⁷. These values suggest that only

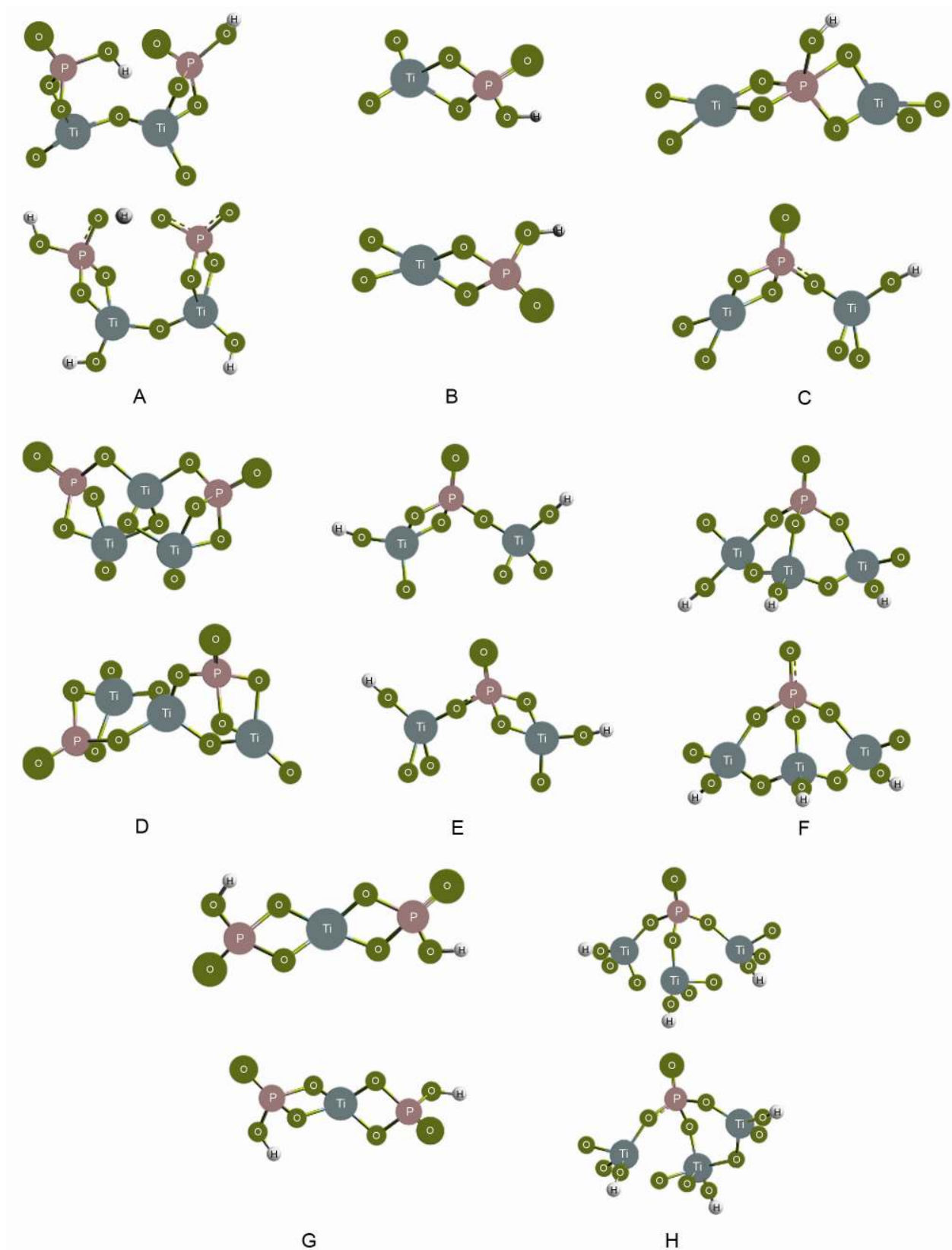


Fig. 1 – Proposed structures of phosphated titania.

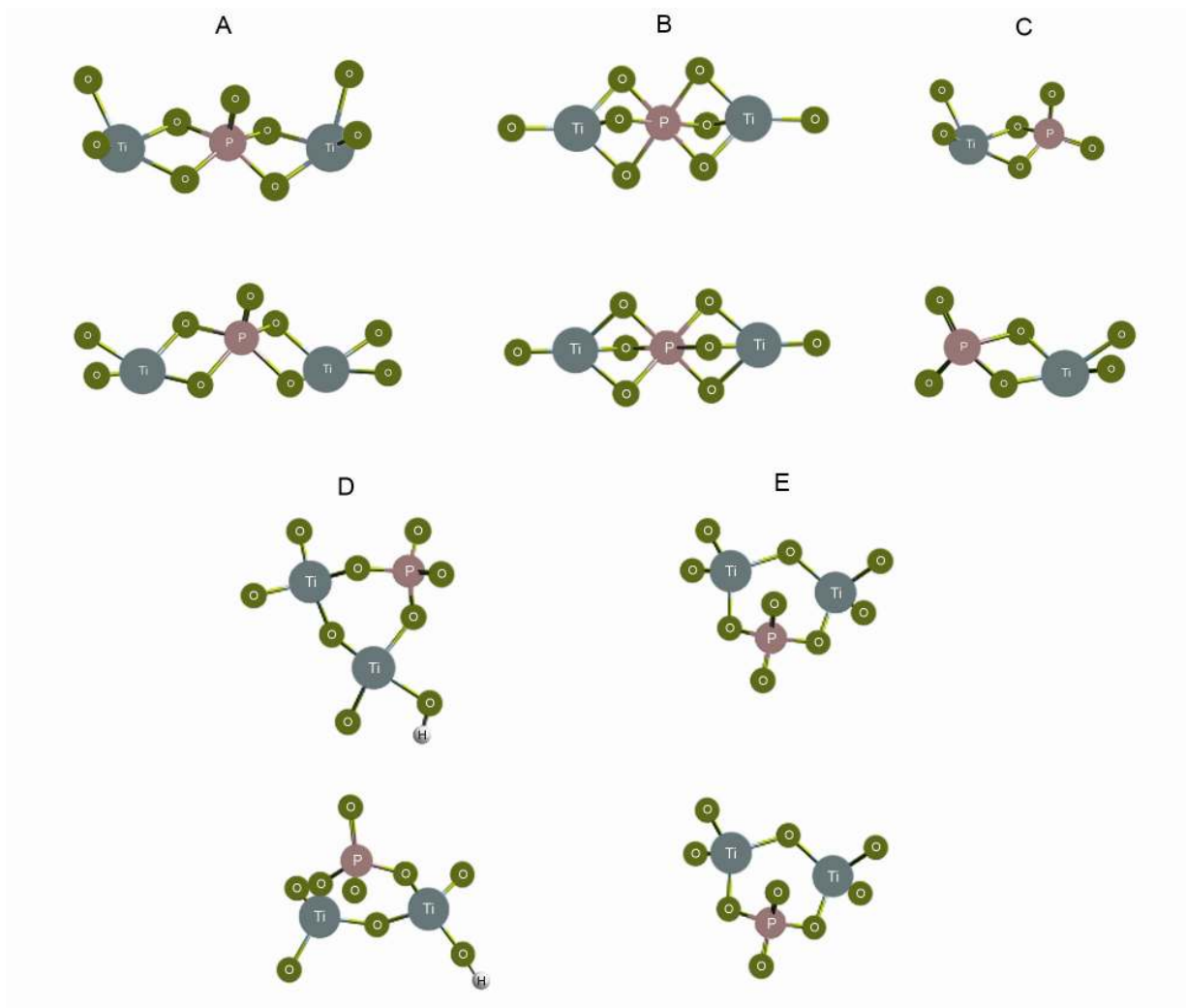


Fig. 2 – Proposed structures of sulphated titania.

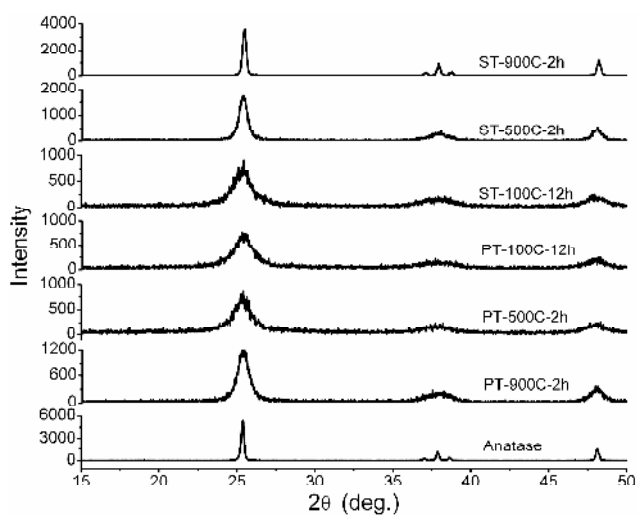
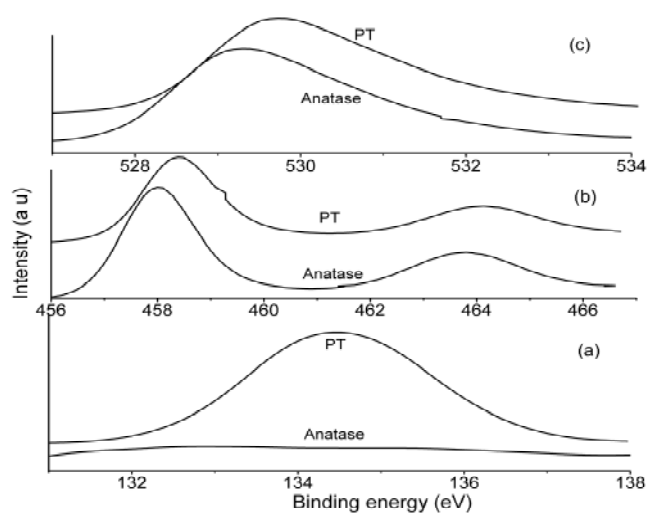


Fig. 3 – XRD patterns of anatase, phosphate modified titania (PT) and sulphated titania (ST) samples calcined at various temperatures.

Fig. 4 – XPS spectra of the (a) $P2p$, (b) $Ti2p$, and (c) $O1s$ taken on phosphate modified titania (PT) and anatase.

PO_4^{3-} is present in PT. However, as the phosphate ions were adsorbed from an acid solution, the presence of free PO_4^{3-} ions in the sample is ruled out. Alternatively, the titanium phosphate formed by the adsorption of PO_4^{3-} ions from phosphoric acid is present in the material either as $(\text{TiO})_2(\text{PO})_2$ or $\text{Ti}(\text{HPO}_4)_2 \cdot x\text{H}_2\text{O}$ ^{38,39}. $\text{Ti}2p_{3/2}$ in PT can be fitted as one peak at 458.4 eV, indicating that Ti ions are in an octahedral environment, coordinated with oxygen³⁷. In the bulk phase of TiO_2 , where Ti ions are in an octahedral environment, only one peak at a binding energy of 458.1 eV is observed. The oxidation state of titanium in PT ($\text{Ti}2p_{3/2}$, binding energy 458.4 eV; $\text{Ti}2p_{1/2}$, binding energy 464.2 eV) does not match with anatase TiO_2 ($\text{Ti}2p_{3/2}$, binding energy 458.1 eV; $\text{Ti}2p_{1/2}$, binding energy 463.8 eV), suggesting the substitution of P in the place of oxygen. The $\text{O}1s$ region of the anatase is composed of a single peak at 529.3 eV, corresponding to the Ti-O in TiO_2 . However, the $\text{O}1s$ binding energy of the PT is observed at 529.7 eV ascribed to the presence of P-O-Ti linkage.

The XPS of the surface of ST are shown in Fig. 5. The S/Ti ratio at the surface of ST was determined to be 0.1. ST exhibits a binding energy for $\text{S}2p_{3/2}$ at 169 eV which is associated with S-O bonds in SO_4^{2-} species⁴⁰, indicating that sulphur in the sample exists in hexavalent oxidation state (S^{6+}) (Fig. 5a). A previous report⁴¹ has assigned the peak at a binding energy of 163 - 164 eV to elemental sulphur or TiS. The absence of this peak for ST reveals the absence of elemental sulphur or TiS in the sample. The binding energy of $\text{S}2p_{3/2}$ at 167.5 eV, is due to SO_3^{2-} species,

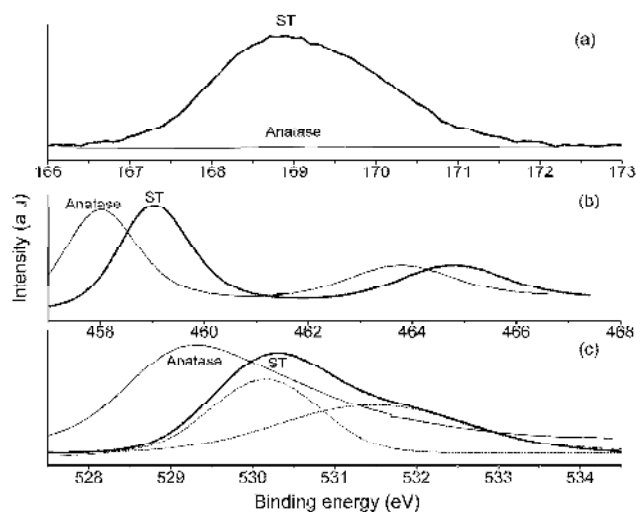


Fig. 5 – XPS spectra of the (a) $\text{S}2p$ (b) $\text{Ti}2p$ and (c) $\text{O}1s$ taken on sulphated titania (ST) and anatase.

the absence of which in ST suggests the absence of sulphite groups in the sample. In addition, the binding energy of 169 eV matches with the $\text{S}2p_{3/2}$ data recorded for $(\text{NH}_4)_2\text{SO}_4$ ⁴². However, as the sulphate ions were adsorbed from an acid solution, the probability of presence of free sulphate ions in the sample is low and explains the anchoring of sulphates on the surface of titania. The peak at a binding energy of 169 eV can be assigned to the bidentately coordinated SO_4^{2-} with the surface Ti^{4+} sites. The XPS for $\text{Ti}2p$ are presented in Fig. 5(b). For pure TiO_2 , a binding energy of 458.1 eV was obtained for $\text{Ti}2p_{3/2}$, referenced to the $\text{C}1s$ at 284.4 eV. The $\text{Ti}2p_{3/2}$ binding energy of the ST sample shifts to a higher value of 459.1 eV, indicating a strong interaction between the sulfate anion and titanium cation with increased positive polarity on the titanium cation. This result is consistent with the model of acid sites on solid superacids of sulfated metal oxides⁴³ shown in Fig. 2. $\text{Ti}2p_{3/2}$ in ST can be fitted as one peak at 459.1 eV, indicating that Ti ions are in an octahedral environment, coordinated with oxygen. The XPS for $\text{O}1s$ are presented in Fig. 5(c). The $\text{O}1s$ for the anatase is composed of a single peak at 529.2 eV, corresponding to the O-Ti-O in TiO_2 . The ST sample shows a shoulder followed by the main peak, which is deconvoluted into another peak as shown in Fig. 5(c). The $\text{O}1s$ binding energy of the ST observed at 530.4 eV is attributed to the presence of S-O-Ti linkage. The deconvoluted peak at a binding energy of 531.7 eV reveals the presence of two different oxygen species in the sample and this could be due to the presence of OH group, S-O bonds or chemisorbed water molecule. From the XPS results, the binding energy of the $2p$ level of Ti in ST at 459.1 eV for $\text{Ti}2p_{3/2}$ and for $\text{Ti}2p_{1/2}$ at 464.7 eV are not in accordance with the binding energies obtained for bulk TiO_2 ($\text{Ti}2p_{3/2}$ at 458.1 eV and $\text{Ti}2p_{1/2}$ at 463.8 eV) suggesting the substitution of sulphate for oxygen in the titania lattice.

IR spectra

The DRIFT spectra of the samples measured in the range of $600\text{-}1200\text{ cm}^{-1}$ are presented in Fig. 6(i). The PT dried at $100\text{ }^\circ\text{C}$ shows characteristic absorption peaks in the range of $600\text{ - }1200\text{ cm}^{-1}$ which is characteristic of phosphate groups resulting from the lowering of symmetry and also due to the adsorption of phosphate ions on the surface of titania⁴⁴.

Although the DRIFT spectra can determine the structure for ST and PT as bidentate, it cannot further

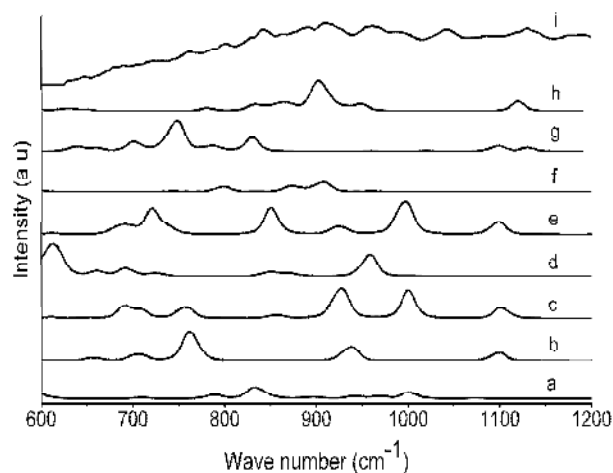


Fig. 6 – (a) – (h) IR absorptions of the phosphated titania structures (A) – (H) obtained by DFT studies; (i) DRIFT spectra measured for phosphated titania.

distinguish the structure as chelating or bridged bidentate since the point group for both the structures are C_{2v} . Similarly, XPS determined the oxidation state for S and P and in addition showed the change in environment for Ti and O present in PT and ST. Hence it appears that the determination of appropriate structures namely monodentate, bidentate or polydentate complex for PT and ST seems to be not possible by experimental tools alone and subsequently the various possible structures were optimized by DFT. The IR absorptions obtained for the DFT optimized structures were evaluated with the DRIFT spectra measured for PT and ST samples. The IR absorptions obtained for that structure which virtually is the same as that of DRIFT spectra of the sample was ascertained as the appropriate structure for PT and ST.

While comparing the theoretical IR absorptions and experimental DRIFT spectra, the intensities of the peaks obtained for DFT studies appear to be significant as the concentration of phosphates or sulphates is only about 5 wt.% in the phosphated and sulphated titania samples.

DFT studies on the structures of phosphated and sulphated titania

The various possible structures of PT are optimized with DFT studies and are shown in Fig. 1. The optimized structure for 'A', shown in Fig. 1 exhibits, two chelating bidentate phosphates attached to the terminal position of titania. The structure endured some modification during the optimization process with the removal of one of the surface hydroxyl

groups attached with the phosphate, which consequently led to the formation of transient bonds between the atoms of phosphorus and oxygen. The optimized structure B obtained for PT shows that the hydroxyl groups are retained on the surface of phosphates as P-O-H when the phosphate group is attached at the surface terminal position of titania. The optimized structure C obtained for PT demonstrates that it is different from the given input structure. The optimization of the structure shows the relocation of hydroxyl groups from the surface of phosphate to titania which may be due to energy constraints. This may well be true when the phosphate is located between two titania groups. In addition, the structure was found to undergo a modification in itself to stabilize with one chelating structure with the input as two chelating structures; this could yet again be due to energy restrictions for the input structure. In structure D, the possible combination of chelating and bridged bidentate was studied. The optimized structure does not reveal any difference with the input structure. The structure E of PT is similar to the optimized structure of 'C' obtained for PT. The difference observed between the input and output is that a transient second bond is formed between the atoms of P and O. In structure F, one phosphate group is attached to three titania groups, forming two bridged bidentate units. There is no difference observed between the structures of input and output. Structure G shows that two phosphate units are connected to one titanium ion and forming two chelating bidentate units. This on DFT optimization not showed any change in the structure. Structure H is an example of monodentate phosphate complex formed on the surface of titania since each oxygen of the phosphate is connected to different titanium ions.

The IR absorptions of the PT structures, A - H obtained by DFT studies and the DRIFT spectra measured for PT are shown in Fig. 6. The theoretical IR absorptions obtained for the PT structures A and D as shown in Fig. 6 (a) and (d) explain the minimum intensities of IR absorption peaks and its non-matching with the experimentally determined DRIFT spectra shown in Fig. 6(i). The dipole moments calculated by DFT for the PT structures show a maximum of 6.87 D for the structure F, which however demonstrates minimum IR absorptions in the region of 600 – 1200 cm^{-1} . The output structures for 'C' and 'E' are the same but show variation in dipole moment; 4.5 D for 'C' and 2.1 for 'E'. Consequently

a reasonable explanation could not be drawn for establishing the structure for PT using dipole moment values. The IR spectra of structure B [Fig. 6(b)], is similar with that obtained for structure C [Fig. 6(c)]. However, the IR data obtained for structures C and E [Fig. 6(c) and (e)] which show resemblance with the experimentally determined DRIFT spectra and further demonstrates that the possible structure of PT could be either 'C' or 'E'. The IR absorptions obtained for structure F [Fig. 6(f)] shows minimum vibrations and hence the monodentate structure formation of phosphate on the surface of titania is not found to be feasible. Although, structure G shows more IR absorptions, there are no absorption peaks in the range of 900 – 1100 cm^{-1} , indicating that may not be the appropriate structure for PT. Structure H shows fewer IR absorptions than structure E and C. Hence, this study confirms a combination of monodentate and chelating bidentate complex (structure C and E), appropriately named as μ -phosphato-bis-(dioxotitanium) complex for the phosphated titania and eliminates the possibility of monodentate or bridged bidentate complex for the PT samples.

The characteristics of sulphate species on the surface of titania was examined by DRIFT spectra. Figure 7(f) shows the DRIFT spectra of the ST sample dried at 100 °C. The DRIFT spectra show the presence of five absorption bands between 930 and 1200 cm^{-1} for the ST sample. A major absorption peak is observed at 1148 cm^{-1} which is generally attributed to asymmetric stretching characteristic of sulphate vibrations^{40,46}. The four other absorption peaks were detected at about 940, 980, 1060, and 1105 cm^{-1} . Furthermore, according to Martin *et al.*⁴⁶ the splitting

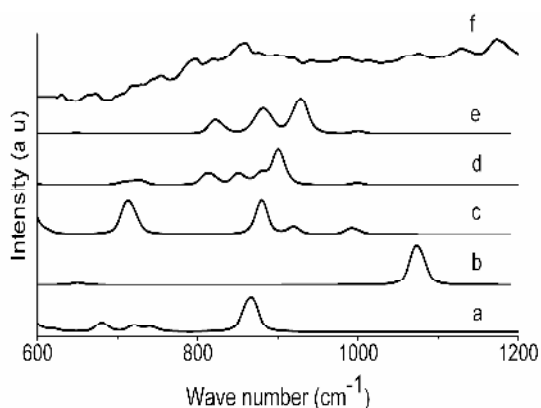


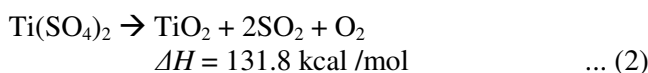
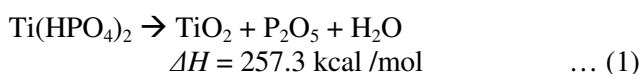
Fig. 7 – (a) – (h) IR absorptions of the sulphated titania structures (A) – (E) obtained by DFT studies; (f) DRIFT spectra measured for sulphated titania.

of the main asymmetric stretching absorption band into three peaks at 1060, 1105, and 1148 cm^{-1} is characteristic of the formation of bidentate sulphate groups. If SO_4^{2-} coordinates to one or two metal ions through two of its oxygen atoms, a chelating (A and C) or a bridged bidentate complex (D) is formed. The reports^{42,45} suggest the characteristic stretching frequencies for ST in the region of 930 - 1200 cm^{-1} . This is in agreement with the XPS data shown in Fig. 5, which indicates a strong predominance of SO_4^{2-} species at the surface of ST. The sulphates at the surface of titania are thought to be mainly in the form of bidentate sulphate groups and show bands at <1400 cm^{-1} . The sulphates start to become polynuclear complex sulphates⁴⁷, possibly of the $\text{S}_2\text{O}_7^{2-}$ and/or $\text{S}_3\text{O}_{10}^{2-}$ type, characterized by absorptions between 1400 and 1600 cm^{-1} . The ST samples synthesized by seeding method contain a maximum of 1.77% sulphur which is equivalent to 5.3% of sulphate. The specific absorption bands were not observed between 1400 and 1600 cm^{-1} for the ST samples indicating the absence of polynuclear sulphates.

The various possible structures of ST are optimized with DFT studies and presented in Fig. 2 (A) - (E). In structure A, the sulphate group is located between two titania groups. Although sulphur can coordinate with six oxygen atoms, in one of the possible structures two of the four oxygen atoms of sulphate are connected to two titanium ions thereby forming two chelating bidentate units as shown in structure A. The optimized structure A shows no change as compared to the input structure. In structure B, the sulphur is coordinated with six oxygen atoms, and each of two titanium ions bonded to three oxygen atoms, thereby forming a polydentate complex. The DFT studies do not show any variation between the input and output structures. The ST is shown as a simple chelating bidentate complex in structure C and bridged bidentate complex in structure D. The output structures do not exhibit any change from the input structure with the DFT optimization showing that the structures are energetically favored. Structure E is similar to structure D. These structures were optimized without hydrogen atoms to study the effect in IR absorption pattern. The IR absorptions obtained for 'E' are similar to those of 'D', although the absorption at 710 – 740 cm^{-1} is not seen for structure E. The IR absorptions of the ST structures, A – E obtained by DFT studies and DRIFT spectra measured for ST are presented in Fig. 7. Figure 7 (a)

and (b) show minimum number of vibrations for the structures in comparison with the DRIFT spectra measured for the proposed structures A and B of Fig. 2. Although the dipole moment for structure A is 10.2 D, this structure does not show many absorption bands in the region of 600 – 1200 cm^{-1} , indicating that 'A' may not be the possible structure for ST. The net change in dipole moment calculated by DFT for the structure B is zero, which further strengthens its inactiveness for IR radiation. In contrast, more vibrations are obtained for the proposed structures C and D as shown in Fig. 7 (c) and (d). The structures C and D show nearly the same dipole moments of 5.19 and 5.02 D respectively. Although structure C shows more intense peaks than 'D', it is structure D which shows more absorption peaks in the range of 600 – 1200 cm^{-1} , indicating that the structure could be bridged bidentate for ST.

The enthalpy of decomposition calculated for ST and PT by DFT (Eqs 1 and 2) shows that the decomposition energy required for hydrated titanium phosphate is greater than that for titanium sulphate. Nevertheless the crystallinity data obtained by XRD for PT at 900 °C shows the energy required for the decomposition of PT to be a few magnitudes greater than that calculated by DFT, which may be attributed to the dissimilarity in structure for PT and ST.



The bond lengths of PT (E) and ST (D) samples (Eqs 1 and 2) obtained by DFT studies show insignificant difference in bond lengths for Ti-O-P and Ti-O-S linkages. However, the greater thermal stability of PT than ST may be attributed to the number of such linkages present in the sample. In PT, there are three Ti-O-P linkages in contrast to the two Ti-O-S linkages in ST. The Mulliken charges obtained for structure E of PT shows the Mulliken charge for 6P as 1.510 and that for oxygen atoms 5O and 4O as -0.693 and -0.697 respectively. Similarly structure D of ST shows Mulliken charge for 6S as 1.346 and oxygen atoms 5O and 9O as -0.684 and -0.677 respectively. The Mulliken charge calculated for Ti in both ST and PT structures shows a charge of 1.344. These observations reveal that the Mulliken charge on the oxygen is more negative in PT than in

ST. In addition, the Mulliken charge is more positive on P than on S showing that the Ti-O-P linkage is stronger than Ti-O-S linkage. This could be one of the possible reasons for the greater thermal stability of PT than ST.

Although there are several synthesis and catalytic studies on phosphated titania and sulphated titania, fewer theoretical studies have been performed on such model systems. The present work is focused on the systematic study on the structures of phosphated and sulphated titania with XRD, XPS, IR spectra and DFT / B3LYP / Lanl2DZ. The XRD patterns measured for PT and ST show that the as-synthesized materials are amorphous in nature. The DRIFT spectra obtained for PT and ST show the presence of bidentate complex in the ST and PT samples. The XPS data for ST and PT show the presence of Ti-O-S and Ti-O-P linkage in ST and PT respectively. The greater thermal stability of PT over ST could be due to the presence higher number of Ti-O-P linkages in PT than Ti-O-S linkages in ST. Among the monodentate, bidentate and polydentate structures studied by DFT for PT and ST, the most probable structure of bridged bidentate for sulphated titania and a combination of monodentate and chelating bidentate for phosphated titania are deduced from the IR absorption obtained by DFT studies.

Acknowledgement

The authors acknowledge the Department of Science and Technology, Government of India for funding the National Centre for Catalysis Research (NCCR) at IIT-Madras, Chennai. Thanks are also due to M/s. Shell India (P) Limited for a fellowship to one of the authors (KJAR).

References

- 1 Diebold U, *Surf Sci Rep*, 48 (2003) 53.
- 2 Breyse M, Portefaix J L & Vrinat M, *Catal Today*, 10 (1991) 489.
- 3 Digne M, Sautet P, Raybaud P, Euzen P & Toulhoat H, *J Catal*, 211 (2002) 1.
- 4 Digne M, Sautet P, Raybaud P, Euzen P & Toulhoat H, *J Catal*, 226 (2004) 54.
- 5 Arrouvel C, Digne M, Breyse M, Toulhoat H & Raybaud P, *J Catal*, 222 (2004) 152.
- 6 Arrouvel C M, Breyse M, Toulhoat H & Raybaud P, *J Catal*, 226 (2004) 260.
- 7 Vittadini A, Selloni A, Rotzinger F P & Gratzel M, *Phys Rev Lett*, 81 (1998) 2954.
- 8 Lazzeri M, Vittadini A & Selloni A, *Phys Rev B*, 63 (2001) 15409.
- 9 Beltran A, Sambrano J R, Calatayud M, Sensato F R & Andres J, *Surf Sci*, 490 (2001) 116.

- 10 Jagdale T C, Takale S P, Sonawane R S, Joshi H M, Patil S I, Kale B B & Ogale S B, *J Phys Chem C*, 112 (2008) 14595.
- 11 Huo Y, Bian Z, Zhang X, Jin Y, Zhu J & Li H, *J Phys Chem C*, 112 (2008) 6546.
- 12 Tang X & Li D, *J Phys Chem C*, 112 (2008) 5405.
- 13 Zhou J K, Lv L, Yu J, Li H L, Guo P Z, Sun H, & Zhao X S, *J Phys Chem C*, 112 (2008) 5316.
- 14 Asahi R, Morikawa T, Ohwaki T, Aoki K & Taga T, *Science*, 293 (2001) 269.
- 15 Umebayashi T, Yamaki T, Itoh H & Asai K, *Appl Phys Lett*, 81 (2002) 454.
- 16 Umebayashi T, Yamaki T, Yamamoto S, Miyashita A, Tanaka S, Sumita T & Asai K, *J Appl Phys*, 93 (2003) 5156.
- 17 Ohno T, Akiyoshi M, Umebayashi T, Asai K, Mitsui T & Matsumura M, *Appl Catal A*, 265 (2004) 115.
- 18 Qiu X & Burda C, *Chem Phys*, 339 (2007) 1.
- 19 Asahi R & Morikawa T, *Chem Phys*, 339 (2007) 57.
- 20 Chen X & Mao S S, *Chem Rev*, 107 (2007) 2891.
- 21 Chen X, Lou Y & Dayal S, *J Nanosci Nanotechnol*, 5 (2005) 1408.
- 22 Oliver, Inderwildi R & Kraft M, *Chem Phys Chem*, 8 (2007) 444.
- 23 Gao H, Zhou J, Dai D & Qu Y, *Chem Eng Tech*, 32 (2009) 867.
- 24 Raghunath P & Lin M C, *J Phys Chem C*, 113 (2009) 8394.
- 25 Fu X, Ding Z, Su W & Chin, *J Catal*, 20 (1999) 321.
- 26 Yu J C, Zhang L, Zheng Z & Zhao J, *Chem Mater*, 15 (2003) 2280.
- 27 Gong W, *Int J Miner Proc*, 63 (2001) 147.
- 28 Fu X, Zeltner W A, Yang Q & Anderson M A, *J Catal*, 168 (1997) 482.
- 29 Saur O, Bensitel M, Mohammed Saad A B, Lavalley J C, Tripp C P & Morrow B A, *J Catal*, 99 (1986) 104.
- 30 Lin L, Lin W, Xie J L, Zhu Y X, Zhao B Y & Xie Y C, *Appl Catal B*, 75 (2007) 52.
- 31 *Gaussian 03, Rev C.02*, 2003, (Gaussian Inc, Wallingford, CT) 2004.
- 32 Becke A D, *J Chem Phys* 98 (1993) 5648.
- 33 Hay P J & Wadt W R, *J Chem Phys*, 82 (1985) 270.
- 34 Joseph Antony Raj K, Ramaswamy A V & Viswanathan B, *J Phys Chem C*, 113 (2009) 13750.
- 35 Splinter S J, Rofagha R & McIntyre N S, *Surf Interf Anal*, 24 (1996) 81.
- 36 Baunack S, Oswald S & Scharnweber D, *Surf Interf Anal*, 26 (1998) 471.
- 37 Zhao D, Chen C, Wang Y, Ji H, Ma W, Zang L & Zhao J, *J Phys Chem C*, 112 (2008) 5993.
- 38 Soria J, Iglesias J E & Sanz J, *J Chem Soc Faraday Trans*, 89 (1993) 2515.
- 39 Hosono H & Abe Y, *J Non Cryst Sol*, 190 (1995) 185.
- 40 Berger F, Beche E, Berjoan R, Klein D & Charbaudet A, *Appl Surf Sci*, 93 (1996) 9.
- 41 Dutta S N, Dowerah D & Frost D C, *Fuel*, 62 (1983) 840.
- 42 Yamaguchi T, *Appl Catal*, 61 (1990) 1.
- 43 Fu X, Zeltner W A, Yang Q & Anderson M A, *J Catal*, 168 (1997) 482.
- 44 Samantaray S K, Mishra T & Parida K M, *J Mol Catal A Chem*, 176 (2001) 151.
- 45 Saur O, Bensitel M, Mohammed Saad A B, Lavalley J C, Tripp C P & Morrow B A, *J Catal*, 99 (1986) 104.
- 46 Martin M A, Childers J W & Palmer R A, *Appl Spec*, 41 (1987) 120.
- 47 Morterra C, Cerrato G, Emanuel C & Bolis V, *J Catal*, 142 (1993) 349.